

## CHAPTER 2

### LITERATURE REVIEW

In this chapter, attention is focused on the perovskite ferroelectrics in the lead zirconate titanate-lead magnesium niobate system. It is first necessary to describe the information background of normal and relaxor ferroelectrics. The relevant literatures on phase formation, microstructure and dielectric properties of PZT, PMN and PZT-PMN are reviewed with attention paid on their processing-microstructure-dielectric properties relationships.

#### 2.1 Perovskite Ferroelectrics

The perovskite structure is specifically characterised by an arrangement of anions and cations similar to  $\text{CaTiO}_3$  where the symmetry of each phase can be quite different. Many ternary compounds of formula  $\text{ABO}_3$  show the perovskite structure, for which the A and B cations differ considerably in crystalline size. While no sublattice is actually close-packed, the structure can be considered as an FCC-derivative structure in which the cation A-layer and oxygen together form an FCC lattice. The smaller B cation occupies the octahedral sites in this FCC array and has only oxygen as its nearest neighbors (Fig. 2.1).

The perovskite family can be  $\text{A}^{2+}\text{B}^{4+}\text{O}_3$  stoichiometry or  $\text{A}^{3+}\text{B}^{3+}\text{O}_3$  stoichiometry, as in  $\text{BaTiO}_3$  (BT) and  $\text{LaGaO}_3$  respectively. Mixed  $\text{A}(\text{B}^{2+}_{1/3}\text{B}^{5+}_{2/3})\text{O}_3$

or  $A(B^{4+}_{1/2}B^{4+}_{1/2})O_3$  compositions are also possible, as found in  $Pb(Mg_{1/3}Nb_{2/3})O_3$  (PMN),  $Pb(Fe_{1/2}Ti_{1/2})O_3$  and  $Pb(Zr_{1-x}Ti_x)O_3$  (PZT).<sup>20</sup> An enormous range of perovskite compositions and solid solutions have been developed for technical applications.<sup>1,21</sup>

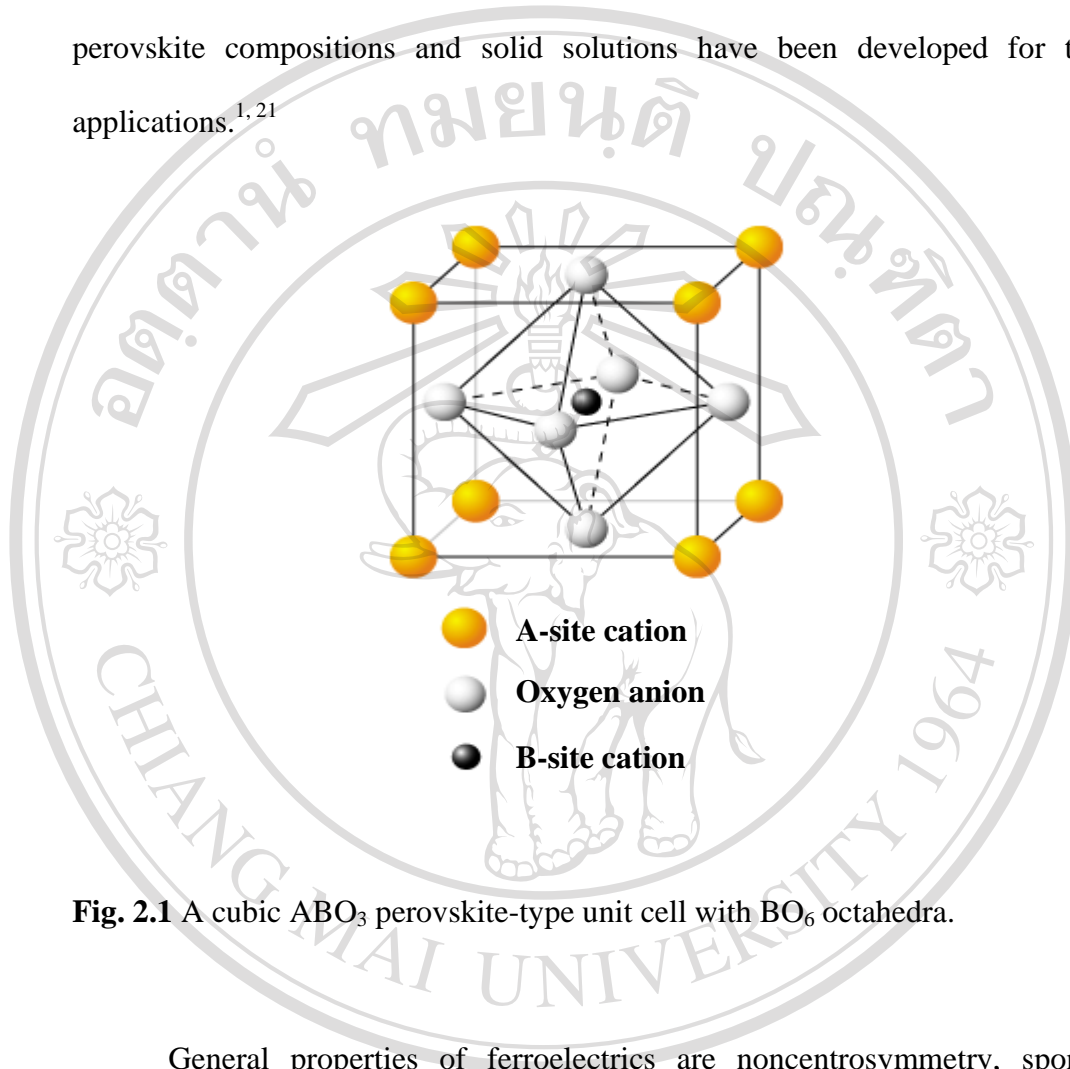


**Fig. 2.1** A cubic  $ABO_3$  perovskite-type unit cell with  $BO_6$  octahedra.

General properties of ferroelectrics are noncentrosymmetry, spontaneous polarization, ferroelectric domains, hysteresis loop, Curie point and phase transition.<sup>22</sup> Hence, ferroelectric ceramics belong to a subgroup of piezoelectric ceramics.

## 2.2 Lead Zirconate Titanate (PZT)

In the early day of technological materials,  $BaTiO_3$  had been predominated, which could date back to the early 1940s. Later, it has been largely supplanted by the PZTs for transducer applications. This is because PZT compositions possess several

more advantages. For example, they exhibit a higher electromechanical coupling coefficients, have higher  $T_c$  values (which permit higher temperatures of operation or higher temperatures of processing during the fabrication of devices), can be easily poled, possess a wide range of dielectric constants, are easier to sinter at lower temperatures and form solid-solution compositions with many different constituents allowing a wide range of achievable properties.

The PZT phase diagram is shown in Fig. 2.2. All compositions are of cubic symmetry above  $T_c$  with the ideal perovskite structure. Below  $T_c$ , as  $Ti^{4+}$  is replaced by  $Zr^{4+}$  in lead titanate ( $PbTiO_3$  or PT), the tetragonal distortion reduces and eventually the structure transforms into a ferroelectric (FE) rhombohedral phase at approximately 47 mole% of PT, the composition termed PZT 53/47 (where 53/47 expresses the Zr:Ti ratio on the B-site). The phase boundary between the two FE phases is almost vertical and thus the transition depends more on composition than temperature. The rhombohedral-tetragonal border is often referred to as the morphotropic phase boundary (MPB). At high  $Zr^{4+}$  content ( $\approx 6$  mol% PT) the orthorhombic antiferroelectric (AFE) structure appears.  $T_c$  progressively decreases as  $Zr^{4+}$  contents increase from pure PT to lead zirconate ( $PbZrO_3$  or PZ). In phase diagram, a second AFE tetragonal phase is shown to exist close to PZ and just below  $T_c$ . Furthermore, the FE rhombohedral phase is divided into a high temperature and a low temperature phases where the distinction lies in the absence of oxygen octahedra tilting in the high temperature phase.<sup>23-25</sup>

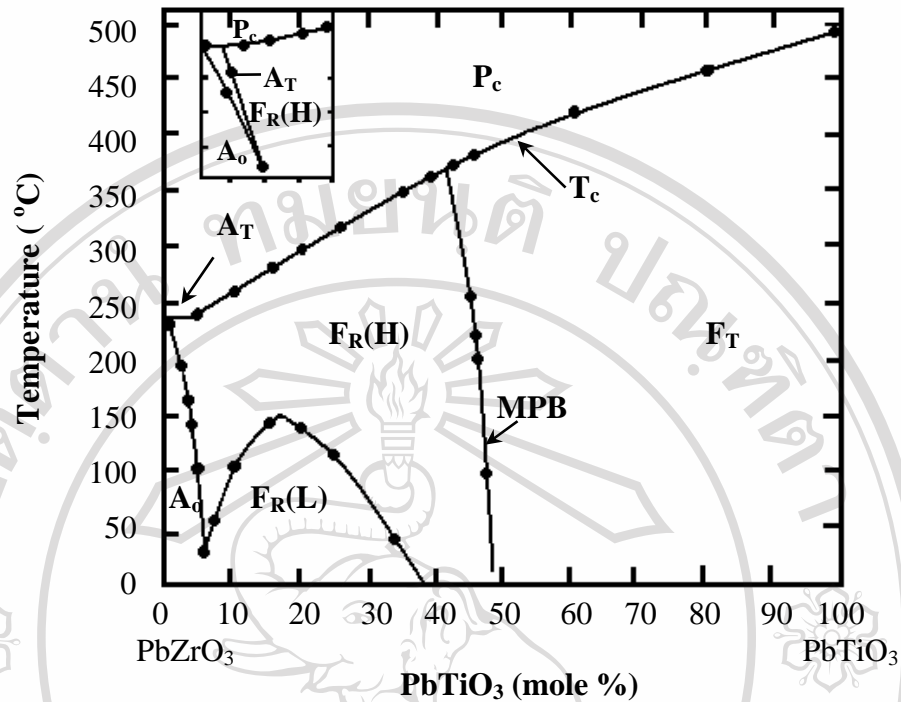


**Fig. 2.2** Phase stabilities in the  $\text{Pb}(\text{Zr}_x\text{Ti}_{1-x})\text{O}_3$  system.<sup>1</sup> (Full descriptions are available in the abbreviations and symbols)

Combination of the two phases, PZ and PT, creates the high temperature pseudo-binary phase diagram for the melting of the PZ-PT solid solution as shown in

Fig. 2.3. The solid solution changes from congruent (PT) to incongruent (PZ) melting at 1340 °C. Also, at high temperature a two-phase region of liquid plus  $\text{ZrO}_2$  is seen to

coexist suggesting the formation of PZT solid solution. Thus, the diagram should be treated as a ternary rather than a pseudo-binary system.<sup>1</sup> However, the  $\text{PbO-TiO}_2\text{-ZrO}_2$  ternary system is often treated as a pseudo-binary system with the end members

PZ and PT due to special interest in their electrical properties.

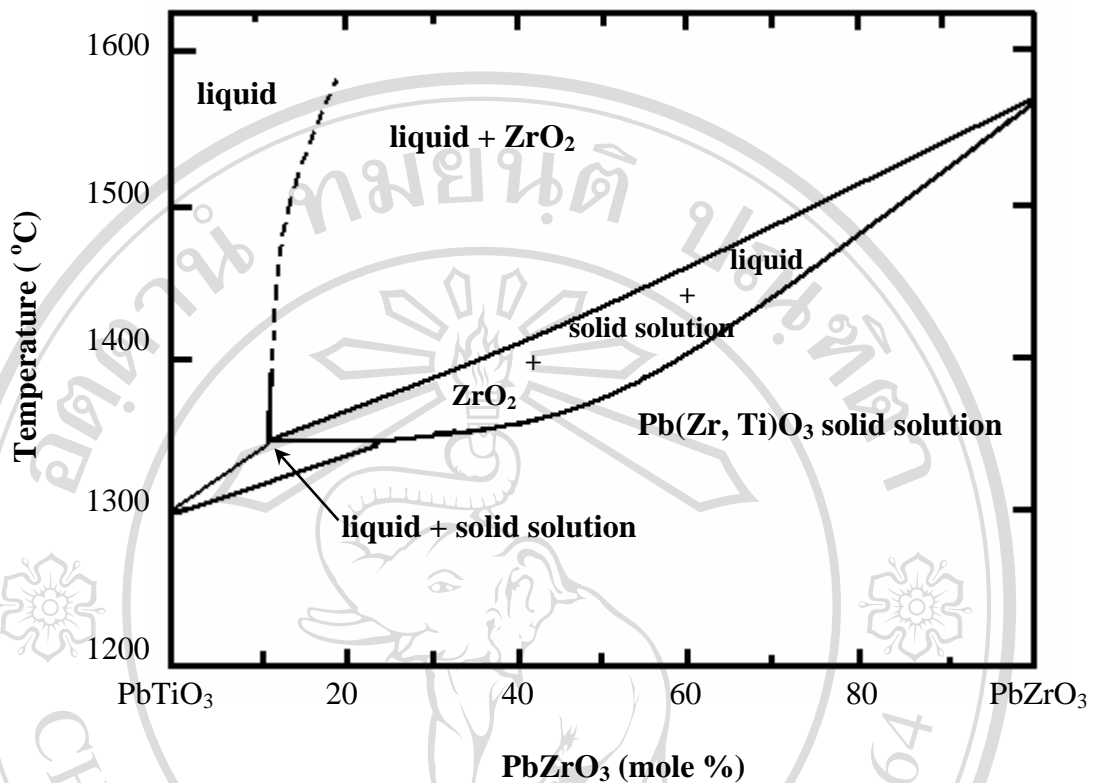


**Fig. 2.3** The high temperature pseudo-binary system of PZ-PT.<sup>1</sup>

The ternary phase diagram PbO-TiO<sub>2</sub>-ZrO<sub>2</sub> at 1100 °C proposed by Jaffe et al.<sup>1</sup> shows another view point (Fig. 2.4). The PZT solid solution exists between 48 and 51 mole % PbO. Depending on the proximity to either or the ZrO<sub>2</sub> and TiO<sub>2</sub> corners the phases ZrO<sub>2</sub>, TiO<sub>2</sub> and ZrTiO<sub>4</sub> exist below 48 mole% PbO. At high PbO contents (> 51 mole %) PZT plus liquid exists at 1100 °C.

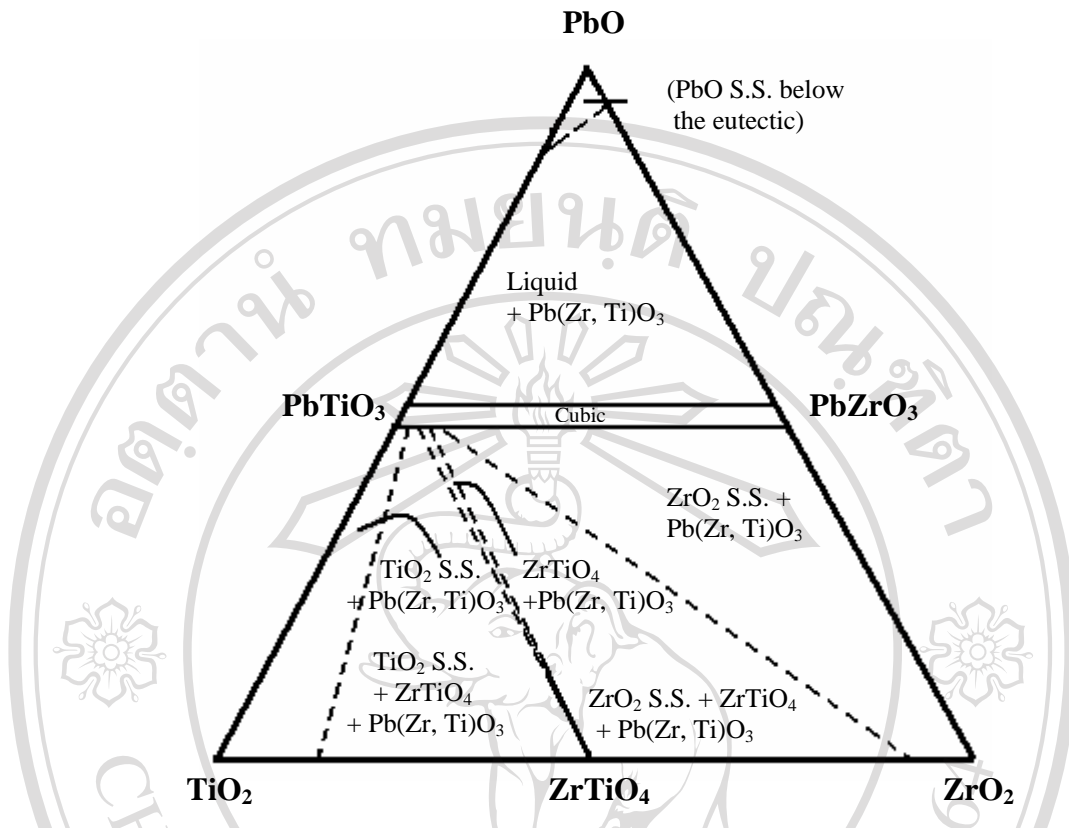


**Fig. 2.4** The ternary system  $\text{PbO-TiO}_2\text{-ZrO}_2$  at  $1100\text{ }^\circ\text{C}$ , where S.S. = solid state.<sup>1</sup>

The nature of the  $\text{PbO-TiO}_2\text{-ZrO}_2$  reaction sequence during formation of PZT was first proposed by Matsuo and Sasaki<sup>26</sup> in the system  $2\text{PbO-TiO}_2\text{-ZrO}_2$ . From the information of XRD experiment, four regions of formation were recognised (as shown in Fig. 2.5).<sup>27-29</sup> In region I, no reactions of the three oxides were detected. Region I changes to region II at  $540\text{ }^\circ\text{C}$  where reaction A:  $\text{PbO} + \text{TiO}_2 \rightarrow \text{PbTiO}_3$  takes place. At  $650\text{ }^\circ\text{C}$  region II converts to region III as  $\text{TiO}_2$  disappears and the reaction B:  $\text{PbTiO}_3 + \text{PbO} + \text{ZrO}_2 \rightarrow \text{Pb(Zr,Ti)O}_3$  takes place. As  $\text{PbO}$  and  $\text{ZrO}_2$  disappear, region III changes to region IV at about  $710\text{ }^\circ\text{C}$  where remaining  $\text{PbTiO}_3$  reacts with PZT in the reaction C:  $\text{Pb(Zr}_{1-x}\text{Ti}_x\text{)O}_3 + \text{PbTiO}_3 \rightarrow \text{Pb(Zr}_{1-x'}\text{Ti}_{x'})\text{O}_3$  where  $(x < x')$ . At



1200 °C region IV becomes a single PZT phase with complete reaction of  $\text{PbTiO}_3$ . No  $\text{PbZrO}_3$  was seen to be formed in this formation sequence of PZT.

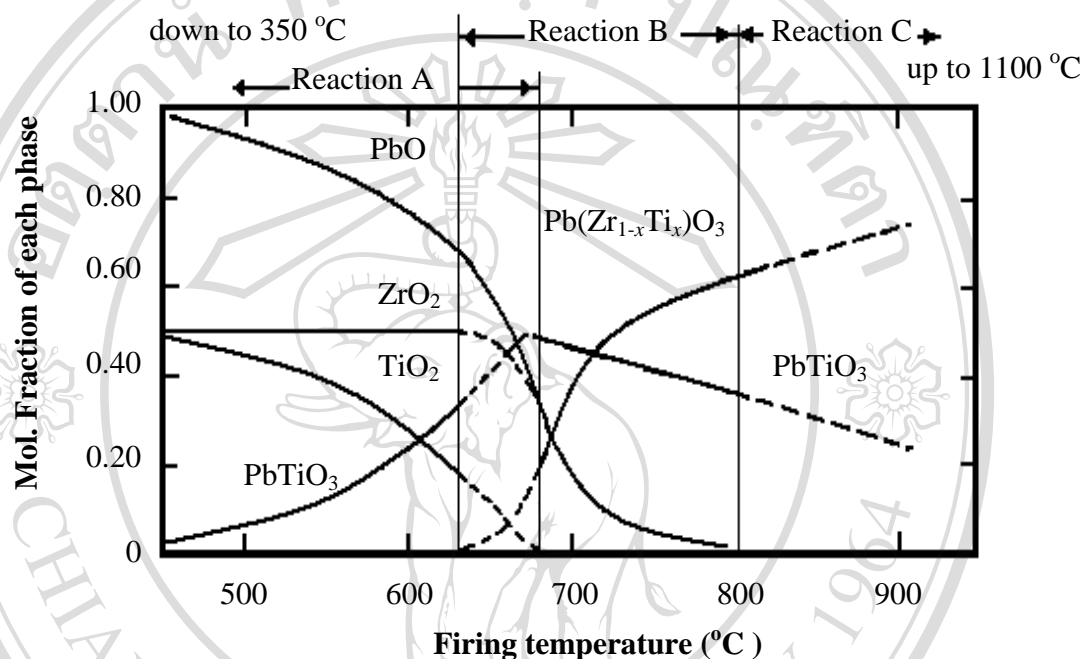


Fig. 2.5 Phases in the system  $2\text{PbO-TiO}_2\text{-ZrO}_2$ .<sup>1</sup>

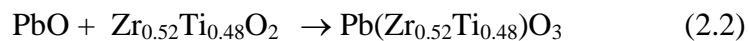
Although other workers agree on the lack of free PZ and the initial formation of PT, discrepancy exists over the actual reaction sequence and phase assemblage during formation. Based on differential thermal analysis (DTA) and X-ray diffraction (XRD), Kingon and Clark<sup>30</sup> reported the formation of a tetragonal solid solution of PZ and PT.  $\text{ZrO}_2$  reacts with PT to form the stoichiometric PZT instead of reaction between PT and an intermediate PZT composition (reaction B) as proposed by Matsuo and Sasaki.<sup>26</sup> Hiremath et al.<sup>31</sup> reported the reaction of two PZT intermediates of different compositions. These were zirconium rich and titanium rich that reacted

with the remaining PT, PbO and ZrO<sub>2</sub>. They also found the discrepancies in the reaction sequence observed by different workers. Such discrepancy was suggested to be due to the difference in raw materials, powder characteristics, mixing methods and other experimental parameters. A tetragonal solid solution was observed in some compositions but was not believed to affect the reaction sequence in the formation of the stoichiometric PZT.

As different raw materials were used, the sequence proposed by Matsuo and Sasaki<sup>26</sup> in Fig. 2.5 was also observed as well as the previously reported sequence. However, all models are the initial formation of PT or a PZT solid solution due to the faster diffusion of Ti<sup>4+</sup> than Zr<sup>4+</sup> at the calcination temperature. This then reacts with the remaining PbO and ZrO<sub>2</sub> to form PZT. Babuskin et al.<sup>32</sup> observed that enhancement of the final properties of the PZT solid solution can be achieved by carrying out the calcination in two steps. In the first step, the B-site oxides are prepared to form a B-site precursor according to the following reactions:



Then, stoichiometric amounts of PbO were added into the B-site precursors to form PZT powder.





These reactions demonstrated a reaction temperature of 720–750 °C to form PZT powders with no phase transition between tetragonal and rhombohedral phases. However, the phase transition of PZT ceramics compositions for piezoelectric applications are usually confined to the vicinity of the MPB as close to this boundary exhibit the highest piezoelectric coupling coefficients as well as maximum relative permittivities. The mechanism resulting in these enhanced properties is believed to be arisen from the coexistence of tetragonal and rhombohedral phases, which gives a total of fourteen possible (pseudo) cubic polarisation directions, six  $\langle 100 \rangle$  in the tetragonal and eight  $\langle 111 \rangle$  in the rhombohedral phases.<sup>12</sup> The large number of polarisation direction enables optimised crystallographic orientations to be established from grain to grain upon poling.

Recently, high-resolution synchrotron X-ray diffraction measurements by Noheda et al.<sup>6, 20</sup> have suggested that an intermediate monoclinic phase exists between the rhombohedral and tetragonal phases in PZT ceramic. The phase transition from tetragonal to monoclinic is reported to be due to the condensation of local Pb which displace in the tetragonal phase along one of the  $\langle 110 \rangle$  directions. The monoclinic unit cell is doubled with respect to the tetragonal one and has  $b$  as the unique axis.  $a_m$  and  $b_m$  are directed along the (pseudo) cubic  $[\bar{1}\bar{1}0]$  and  $[1\bar{1}0]$  directions<sup>5</sup>, respectively, while  $c_m$  is close to the tetragonal  $c$  axis, along the  $[001]$ , but tilted away from it. Such that, the angle  $\beta$  between the  $a_m$  and  $b_m$  is slightly larger than  $90^\circ$ . This monoclinic phase has unique characteristics in comparison to all other ferroelectric perovskite phases. The polar axis is not determined by the symmetry and can be directed anywhere within the monoclinic  $ac$  plane; that is, the polar axis is allowed to rotate within this plane. In this case, the (pseudo) cubic  $[111]$  and  $[001]$  directions are

contained within the monoclinic plane and the monoclinic polar axis is tilted away from the polar axis of the tetragonal phase [001] towards to that of the rhombohedral phase [111]. Noheda et al.<sup>6, 33</sup> also proposed that the presence of this monoclinic distortion is the origin of the unusually high piezoelectric response in the vicinity of the MPB in PZT. The observation of this monoclinic phase has allowed a preliminary modification of the PZT phase diagram (Fig. 2.6).

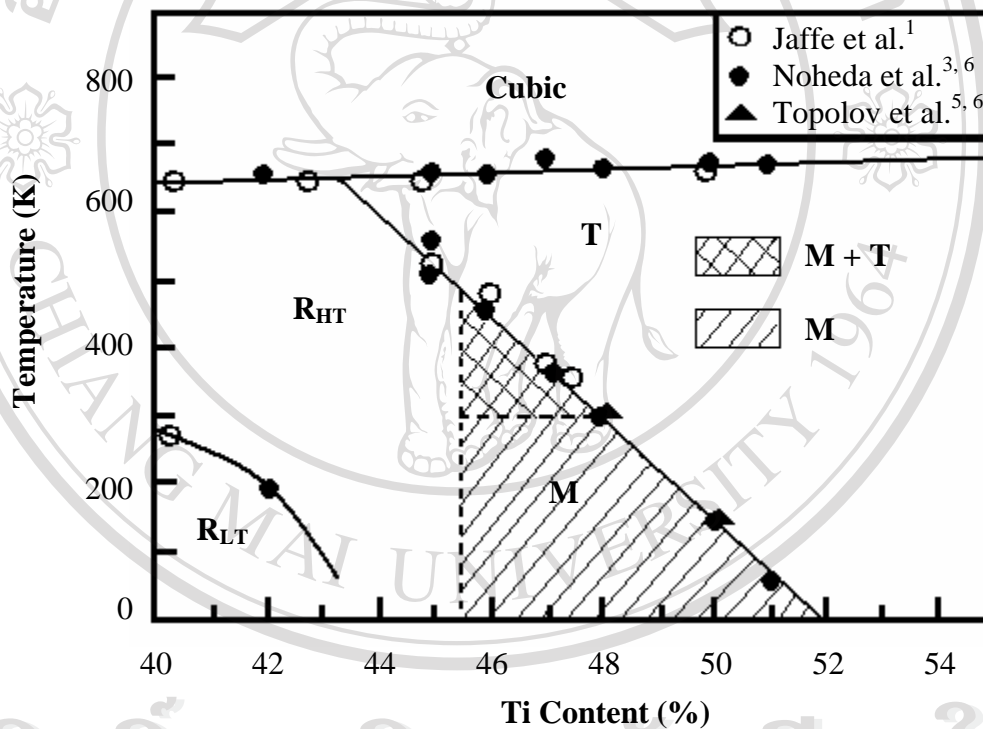
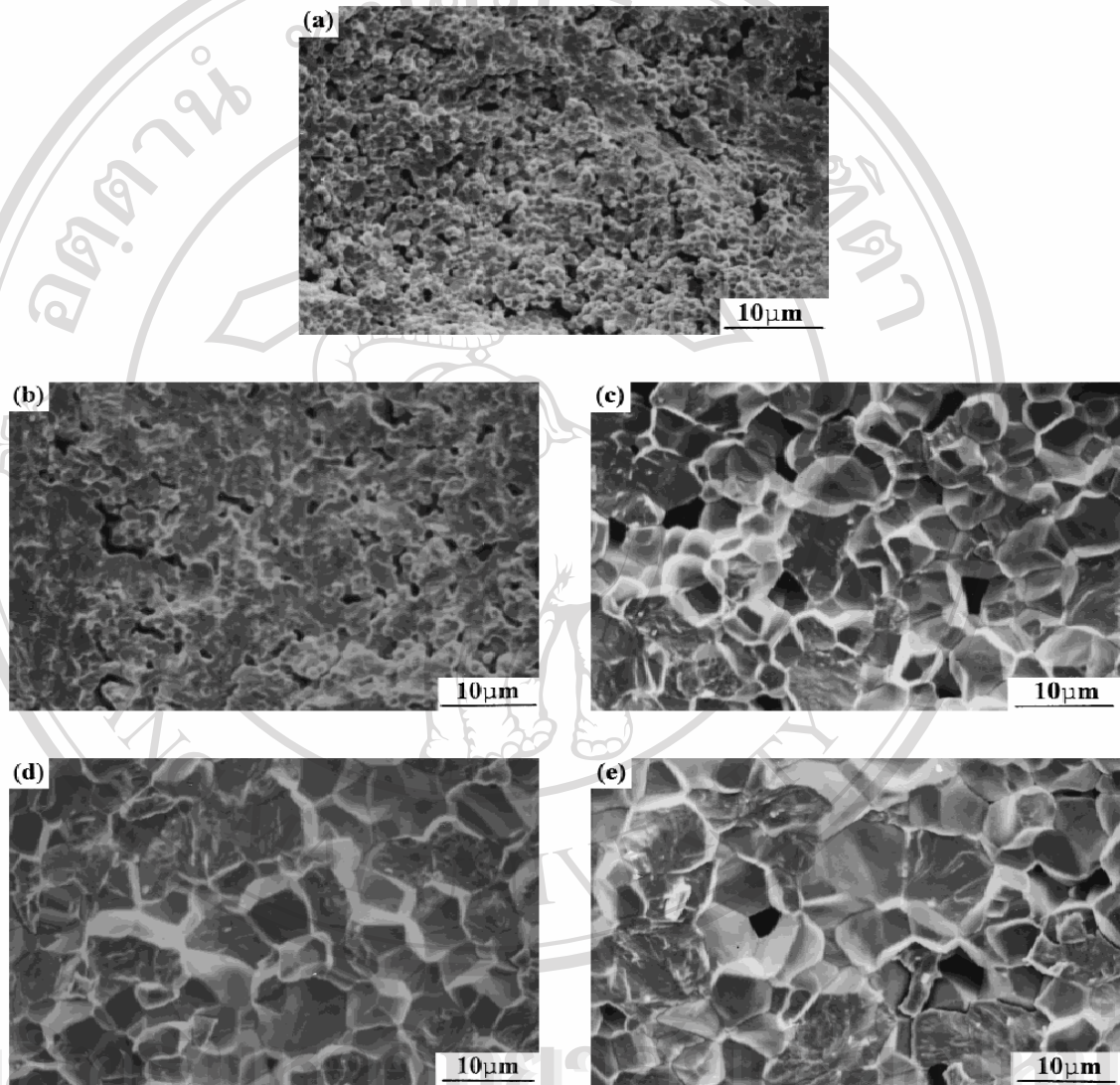


Fig. 2.6 PZT phase diagram around the MPB proposed by Noheda et al.<sup>6, 34</sup>

PZT compositions are commonly sintered at high temperatures in the range 1100-1300 °C. This creates problems with vaporisation of PbO during sintering and possible lead deficiency which may cause segregation of a ZrO<sub>2</sub> phase. This may

affect the electrical properties of the material. PbO atmosphere control thus becomes one of the important parameters in the processing of PZT.



**Fig. 2.7** Fracture surface of PZT ceramics sintered at (a) 950 °C, (b) 1000 °C, (c) 1050 °C, (d) 1100 °C and (e) 1150 °C.<sup>35</sup>

To prevent PbO loss during sintering, an atmosphere of higher PbO partial pressure than that of the materials must be obtained.<sup>30, 36, 37</sup> Hardtl and Rau<sup>36</sup> found

that at all measured temperature PZ had the highest PbO vapour pressure when compared to any other PZT compositions. They concluded that any firing of PZT materials should be conducted in covered crucibles with the addition of PZ pellets to maintain a PbO pressure higher than the dissociation pressure of the sintered PZT composition.

To compensate for the lead loss in the samples, some excess PbO is usually added during batch preparation.<sup>30, 37</sup> Sintering is also carried out in the presence of atmospheric powders so that the lead activity of the PZT sample (defined as the ratio of PbO vapor pressure above the PZT compound to the PbO vapor pressure above pure PbO at a given temperature) and the surrounding atmosphere are nearly the same. However, any deviation in the lead activity of the atmospheric powder results in adsorption or loss of PbO to or from the atmosphere. Depending on whether PbO is in excess or short of the stoichiometry, a PbO rich liquid phase or a ZrO<sub>2</sub> phase may be formed in the PZT sample. The optimum sintering temperature was taken as the point when the PbO vapor pressure evaporation-recondensation equilibrium for the reaction:  $\text{PbO-PbO (vapor)} + \text{Pb (vapor)} + \frac{1}{2} \text{O}_2$  was established.<sup>38</sup>

The microstructure of ceramics included factors such as grain size, grain boundary, density, porosity, homogeneity and etc. In general, the grain size of PZT ceramics increases with the sintering temperature and dwell time (Fig. 2.7).<sup>37, 39</sup> Most commercial piezoelectric disks are sintered to about 96 to 97 % of theoretical density and have grain sizes between 2 to 10  $\mu\text{m}$ . It is well-known that grain size and bulk density markedly influence the electrical characteristics of sintered piezoelectric ceramics. By using hot-pressing technique, one should be able to control the grain growth and densification processes and yields about 99% dense ceramics with

controlled grain size suitable for the extreme thinning required for high frequency applications.<sup>40</sup>

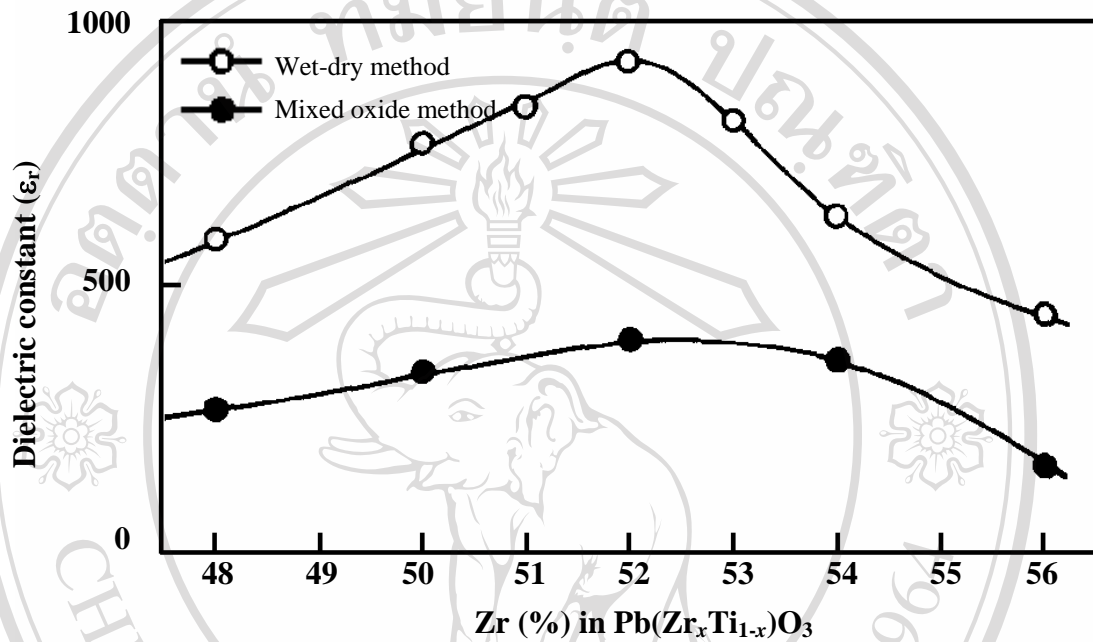


**Fig. 2.8** Dependence of dielectric constant of PZT ceramics on chemical compositions at room temperature.<sup>41</sup>

Kakegawa et al.<sup>41</sup> reported that the dielectric constant of PZT ceramics depends on their chemical compositions. As shown in Fig. 2.8, the dielectric constant near  $x = 0.52$  of PZT ceramics rises sharply against those of the other compositions.

Jin et al.<sup>42</sup> reported that the maximum dielectric constant and transition temperature of  $\text{Pb}(\text{Zr}_{0.52}\text{Ti}_{0.48})\text{O}_3$  ceramics increased as the grain size decreased. However, Surowiak et al.<sup>43</sup> pointed out that the smaller grain size of  $\text{Pb}(\text{Zr}_{0.52}\text{Ti}_{0.48})\text{O}_3$  ceramics does not show a good dielectric and piezoelectric properties. It has been suggested that the deterioration of the piezoelectric properties with decreasing grain size is probably



related to the effects of fewer domains and less mobile domain walls. Some researchers<sup>44, 45</sup> observed that the domain structures formed at the paraelectric-ferroelectric phase transition are strongly dependent on the elastic boundary conditions and crystallite sizes. The fine grains have simple domain structures implying a reduction in the degrees of freedom and a fine grain can readily deform. The reduced variants combined with the surface pinning of the domain walls may become the origin for the reduction of domain wall mobility (extrinsic contribution) and hence the associated extrinsic dielectric properties for the PZT ceramics. Sintering in oxygen atmosphere is reported to facilitate the pore-elimination process.<sup>43</sup> The PZT ceramic possesses higher densities and grain growth is suppressed with an increase of the oxygen partial pressure.

Homogeneity is found to have a profound effect on the piezoelectric properties regardless of density and grain size. Kim et al.<sup>46</sup> reported that for the same PZT composition prepared via different processing routes, the electrical characteristics are entirely different. PZT ceramics processed via the conventional mixed-oxide route possessed significantly lower dielectric and piezoelectric properties than those processed via the reactive calcination. This difference reflects the effect of inhomogeneity in the PZT compositions on their properties and is dependent on the Zr/Ti ratio near the MPB. Also the piezoelectric properties for the latter materials sintered at 1000 °C are inferior to those sintered at 1200 °C though having similar densities and grain sizes. The lower values are believed to be related to the crystallinity of materials being less developed. The associated defects thus result in a stiffening out of the extrinsic polarisability (domain wall motion).<sup>44</sup>



### 2.3 Lead Magnesium Niobate (PMN)

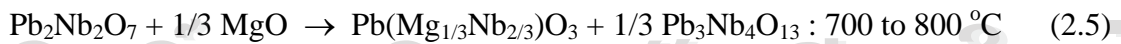
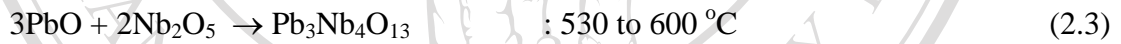
Relaxor ferroelectric is a class of lead-based complex perovskites with the general formula  $\text{Pb}(\text{B}_1\text{B}_2)\text{O}_3$  where  $\text{B}_1$  is a lower valency cation (e.g.  $\text{Mg}^{2+}$ ,  $\text{Zn}^{2+}$ ,  $\text{Ni}^{2+}$ ,  $\text{Fe}^{3+}$ ) and  $\text{B}_2$  is a higher valency cation (e.g.  $\text{Nb}^{5+}$ ,  $\text{Ta}^{5+}$ ,  $\text{W}^{5+}$ ). Pure lead magnesium niobate (PMN)<sup>47, 48</sup> is a representative of this class of materials with a Curie point of  $-10\text{ }^\circ\text{C}$ , at 1 kHz. Relaxor can be distinguished from normal ferroelectrics by the presence of a diffuse phase transition (DPT) on cooling below the Curie point. It has been postulated that the broadening of its  $T_c$  range is attributed to the compositional fluctuations within the material.<sup>48</sup> Some regions in the relaxor may contain different chemical compositions with different  $T_c$ . Consequently, the observed result is an overall broadening of  $T_c$ . Each of these micro/nano polar-regions are characterised by a normal first-order phase\* transition. The existence of these micro/nano regions in the ceramics have been attributed to cation disorder or fluctuations within the B-site of  $\text{A}(\text{B}_1\text{B}_2)\text{O}_3$ . For example, there is cation disorder in the B-site for  $\text{Pb}(\text{Mg}_{1/3}\text{Nb}_{2/3})\text{O}_3$ .<sup>46, 49, 50</sup> The composition regarding Mg/Nb ratio is not stoichiometric in the micro/nano-regions, leading to different ferroelectric transition temperatures which enhances the dielectric peak broadening. However, there have been many models proposed to explain the behavior of the relaxor ferroelectric, for example, the inhomogeneous micro/nano-region model, the micro-micro domain transition model, the superparaelectric model, the dipolar glass model, the order-disorder model and etc.<sup>48-53</sup>

---

\* The polarization changes abruptly, to zero at the transition temperature.<sup>1</sup>

The relaxors also show a very strong frequency dependence of the dielectric constant. The Curie point shifts to higher temperatures with increasing frequency. The dissipation factors are highest just below the Curie point. For PMN relaxors which have a second-order phase transition\*. Levstik et al.<sup>54</sup> have demonstrated that its relaxation spectrum and temperature characteristics exhibit remarkable similarities to dipolar glasses.

From Inada's work<sup>55</sup>, it is clear that the formation of perovskite PMN is directly related to the reactivity of the oxide MgO (or in the case of other relaxors the B<sub>1</sub>-site cations), relative to that of other phases in the binary system PbO-Nb<sub>2</sub>O<sub>5</sub> (Fig. 2.9). The formation of perovskite PMN powder with the repetition of the following reactions (eq. 2.3 to 2.5) is given below.



The initial reaction between PbO and Nb<sub>2</sub>O<sub>5</sub> results in the formation of cubic pyrochlore (Pb<sub>3</sub>Nb<sub>4</sub>O<sub>13</sub> or P<sub>3</sub>N<sub>4</sub>), where upon further reaction with PbO results in the formation of a rhombohedral pyrochlore Pb<sub>2</sub>Nb<sub>2</sub>O<sub>7</sub> (P<sub>2</sub>N<sub>2</sub>). The rhombohedral pyrochlore then reacts with MgO at higher temperature to form perovskite PMN, with

\* The polarization goes continuously to zero at the transition temperature (or beyond T<sub>C</sub>).<sup>1</sup>

the reappearance of cubic pyrochlore phase. Thus, to obtain single-phase PMN, it is necessary to prevent the evaporation of PbO, which would slow down these reactions, and to repeat the process of crushing, and calcination. This reaction sequence is also similar to that proposed for PFN.<sup>56</sup>

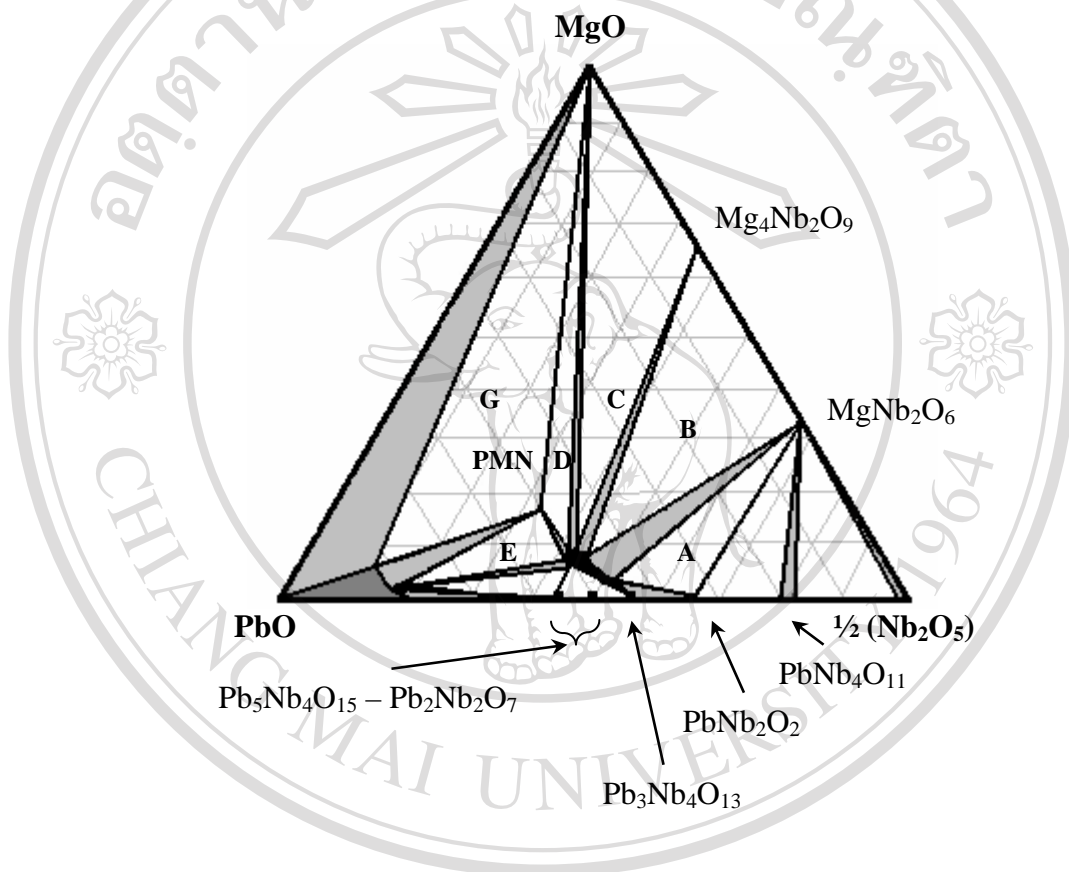


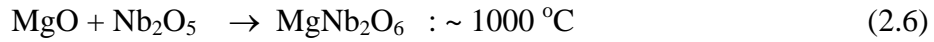
**Fig. 2.9** Ternary phase diagram of the PbO-MgO-Nb<sub>2</sub>O<sub>5</sub> system at 1000 °C. The black domain represents the pyrochlore (Py) solid-solution range, the light gray area corresponds to diphasic domains, and the dark gray area represents the extent of the liquidus at 1000 °C.<sup>57</sup>

Lejeune and Boilot<sup>58</sup> have reported a somewhat different reaction sequence for the formation of PMN and PFN. They have found that the reaction of PbO and Nb<sub>2</sub>O<sub>5</sub>

leads to the formation of three types of pyrochlore phases,  $P_2N_2$  and  $P_3N_4$  and further reaction between  $P_2N_2$  with PbO forms a lead-rich  $P_2N_2$  pyrochlore with the  $P_3N_4$  cubic pyrochlore phase being stable. At about 830 °C, a liquid phase was found to form and  $P_2N_2$  reacted with MgO to form perovskite PMN with the  $P_3N_4$  phase being unaltered.

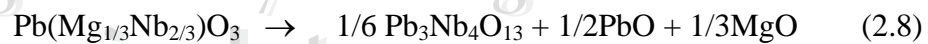
Another interesting reaction sequence for the formation of PMN was also introduced by Swartz and Shrout.<sup>19</sup> In their work, only the cubic pyrochlore  $P_3N_4$  was observed, which in turn reacted with PbO and MgO to form perovskite PMN. They also confirmed that MgO was incorporated into the cubic pyrochlore structure having an approximate formula of  $Pb_{1.83}Nb_{1.71}Mg_{0.29}O_{6.39}$ . The exact amount of MgO that can be incorporated into the pyrochlore structure is not yet known. Several researchers<sup>16, 47, 59</sup> have also reported the partial incorporation of MgO in the pyrochlore phase with a similar composition. These literature indicated that PMN does not form by a direct reaction of the oxides but by subsequent reactions through pyrochlore phases, therefore, the cubic pyrochlore is very stable and is never completely eliminated. Also, the formation of PMN could be accelerated by addition of excess PbO and MgO.<sup>16, 59</sup> Different reaction sequences in the formation of PMN could be due to the dependence of reaction kinetics on various processing parameters, such as particle size and surface area of the raw materials, heat treatment and etc.<sup>19, 59</sup>

To obtain stoichiometric perovskite PMN, the intermediate pyrochlore phases reaction must be eliminated. Thus, a novel approach was devised, whereby the two refractory B-site oxides, MgO and  $Nb_2O_5$ , were pre-reacted to form the columbite  $MgNb_2O_6$  before reaction with PbO as shown:<sup>19</sup>



In this reaction sequence, the pyrochlore formation is bypassed, leading to the direct formation of PMN. Naturally the success of this approach depends on various processing parameters, such as reactivity of MgO, degree of mixing, control of PbO volatility, and the reversibility of reaction (eq. 2.7). It has been confirmed by many researchers<sup>16, 19, 57, 60</sup> that pyrochlore-free PMN phase, can be achieved by employing this method.

Effect of various processing parameters on the composition and amount of phases formed in the preparation of PMN has been investigated by Lejeune and Boilot.<sup>58, 61</sup> Results of various ceramic processing studies are given in Table. 2.1. As expected, reaction sequences (eq. 2.6) through (eq. 2.7), process that reduce the volatility of PbO, such as shorter sintering time and closed crucible firing, lead to an increased amount of perovskite phase. Conversely, process that lead to PbO loss such as prolong firing, leads to an increased amount of pyrochlore phase, as is evident from the following reverse reaction:



From this reaction as well as other reactions in which a pyrochlore phase forms, free PbO will be present in the ceramic unless driven off through volatilization. The presence of free PbO is commonly observed at the grain boundaries and at triple



points. It is believed that this relatively weak amorphous PbO grain boundary phase gives rise to the characteristic intergranular fracture frequently observed in relaxors. Along with the amorphous PbO at the grain boundary, small grains of pyrochlore are also observed. It has been reported that, depending on the ceramic process, a pyrochlore phase can also exist in the form of large discrete grains, as example shown in Fig. 2.10.

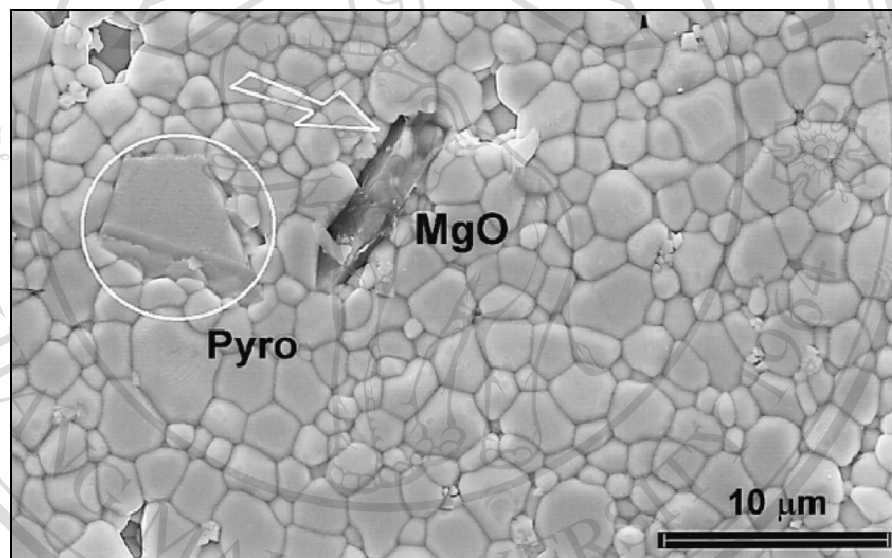


**Fig. 2.10** As-fired surface of PMN ceramic indicating the existence of pyrochlore (Pyro) and MgO phases.<sup>16</sup>

From Table 2.1, it is seen that the reactivity of raw material, firing condition and atmosphere can be modified to enhance the yield of perovskite PMN. To eliminate the pyrochlore phase completely, it has been shown that an addition of up to 6 wt% excess PbO is necessary.<sup>62</sup> Excess PbO accelerates the formation of the PbO rich pyrochlore phases,  $P_2N_2$  and  $P_3N_2$ . The addition of excess MgO (at least 5 mol%)



also helps to eliminate the pyrochlore phase by compensating for poor dispersibility and reactivity.<sup>63</sup> The PMN perovskite phase will be nonstoichiometric, which is not desirable. The importance of obtaining a stoichiometric perovskite PMN composition is evident by the vast variation in physical and dielectric properties reported for PMN in Table 2.2. It is clear that PbO and MgO deficiency can result in an excessive amount of pyrochlore phase which causes poor densification and greatly degraded dielectric properties. Discrete grains of pyrochlore phases ( $\epsilon_r \sim 120$ ) would have little effect on the dielectric properties of relaxor, but presence of free PbO ( $\epsilon_r \sim 20$ ) in the grain boundary will lower the overall dielectric constant, giving rise to the observed grain size dependency of  $\epsilon_r$ .<sup>64</sup>

**Table 2.1** Influence of processing parameters on PMN formation.<sup>61</sup>

Process	Parameter	Perovskite PMN (wt%)	Comment
Raw material	MgO $\rightarrow$ MgCO <sub>3</sub>	42 $\rightarrow$ 81	Improved reactivity
Solvent	Water $\rightarrow$ acetone	51 $\rightarrow$ 81	and dispersability
Calcination	Cycles 1 to 3	60 $\rightarrow$ 90	Help prevent anion deficient pyrochlore formation
	800 $\rightarrow$ 1000 °C Air O <sub>2</sub>	68 $\rightarrow$ 76 77 $\rightarrow$ 85	
Sintering Condition	Dwell time 6 $\rightarrow$ 24 h, at 1050°C, Heating rate 770 $\rightarrow$ 5 °C/min Open $\rightarrow$ close crucible	81 $\rightarrow$ 60 49 $\rightarrow$ 77 33 $\rightarrow$ 80	PbO loss  PbO source

**Table 2.2** Effect of nonstoichiometry on the dielectric properties of PMN ceramics.<sup>65, 66</sup>

Parameter	Effect	Comment
PbO deficiency	Reduction in $\epsilon_r$	Promotes formation of pyrochlore and poor densification
MgO deficiency	Reduction in $\epsilon_r$	Promotes pyrochlore
PbO excess	Reduction in $\epsilon_r$ Insulation resistance (IR) degraded Enhanced $\epsilon_r$ and IR Increase in aging	Excess PbO in grain boundary Promotes densification and perovskite phase
MgO excess	Increase in $\epsilon_r$	Promotes grain growth and elimination of pyrochlore phase

PMN ceramics exhibit a frequency dependent maximum of the dielectric constant around room temperature, generally ascribed to a “diffuse phase transition”, although the mean structure remains cubic down to 5 K.<sup>64</sup> Indeed, no macroscopic phase transition has been observed neither by X-ray diffraction experiments<sup>57</sup> nor by optical birefringence techniques.<sup>67, 68</sup>

Because two types of cations of different ionic size and electrical charge occupy the same crystallographic position, nanoscale ordered regions, characterized by a regular one-by-one alternation of the  $\text{Mg}^{2+}$  and  $\text{Nb}^{5+}$  ions, form during the sintering process.<sup>69</sup> In addition, a displacive ordering in the atomic position due to

ionic displacement has been recently suggested using direct observation of the superlattice X-ray diffraction peaks.<sup>69</sup>

The relaxor properties of PMN are related to these chemical heterogeneities which are known to be strongly dependent on composition modification, due to unwanted defect creation (e.g. lead vacancies) or ion substitution. The presence of correlated polar clusters of rhombohedral symmetry was revealed by the profile analysis of X-ray and neutron diffraction lines.<sup>70</sup> The correlation of the Nb<sup>5+</sup> shifts in the Nb-rich matrix (approximately 0.11 Å in  $\langle 111 \rangle_{\text{cub}}$  direction) was also confirmed by an EXAFS study.<sup>55, 71</sup>

Since the preparation of pure perovskite PMN is relatively difficult via conventional solid state route, in this work, attempt has been made to produce pure, dense PMN ceramics by the modified mixed oxide method. This study was also undertaken to further examine the inter-relationships between processing, phase formation, microstructure and dielectric properties of PMN ceramics.

## 2.4 Lead Zirconate Titanate – Lead Magnesium Niobate

To date, numerous lead-based complex perovskite compounds being proposed for electroceramic applications are based on a wide variety of solid solutions comprised of relaxor and normal type ferroelectric perovskite end member as well as a variety of modifiers.<sup>72</sup> Of particular interest are compositions in the PMN-PT, PMN-PFN, PMN-Pb(Sc<sub>1/2</sub>Nb<sub>1/2</sub>)O<sub>3</sub> (PSN), PMN-Pb(Mg<sub>1/2</sub>W<sub>1/2</sub>)O<sub>3</sub> (PMW) and PMN-PT-PZ systems.<sup>73-75</sup>

Normal type ferroelectric of the PbZrO<sub>3</sub>-PbTiO<sub>3</sub> or PZT solid solution system has been the main material of choice for piezoelectric applications since 1950's. The

specific advantages of PZT ceramics are already described in *Section 2.2*. On the other hand, relaxor type ferroelectrics are typified by lead magnesium niobate (PMN) which exhibits frequency-dependent permittivity maxima, and large frequency-dependent dissipation factor maxima below the Curie temperature as mentioned in *Section 2.3*. Thus, the combination of lead zirconate titanate and lead magnesium niobate or  $x\text{PZT}-(1-x)\text{PMN}$  system should be able to form an alternative material composition for further development and utilization in the area of electroceramics.

The first electrical properties of the PMN-PT-PZ ternary system were investigated by Ouchi et al.<sup>76</sup> They have found that a high dielectric constant was obtained for the compositions near the morphotropic transformation. The possible application as an actuator and piezoelectricity of the  $x\text{PMN}-(1-x)\text{PZT}$  ceramics were also demonstrated by Shaw et al.<sup>77</sup> in 1993.

According to Ouchi et al.'s work, the phase diagram for PMN-PZ-PT system was introduced as shown in Fig. 2.11. The tetragonal phase area is bounded by a convex curve to PT in the present ternary compositions. While the area of tetragonal phase in PT-PZ-PbO compositions are bounded by a concave curve to PT. The difference in these phase boundary shifts is related to ionic radii of the B site ions in a perovskite-type compound but it still cannot be fully explained.

PMN-PZT solid solution with different reaction sequences was also prepared and characterized by Kakegawa et al.<sup>78</sup> For the first sequence, a mixture of PbO, ZrO<sub>2</sub>, TiO<sub>2</sub>, MgO and Nb<sub>2</sub>O<sub>5</sub> (P+Z+T+M+N) was calcined. The presence of the intermediate phase, PbTiO<sub>3</sub>, was found when temperature exceed 800 °C and decomposed at above 1200 °C up to at 900 °C, then PMN-PZT solid solution started to form. For the second sequence, the mixtures of PbO, ZrTiO<sub>4</sub>, MgO and Nb<sub>2</sub>O<sub>5</sub>

(P+ZT+M+N) was calcined. By this reaction, PMN-PZT solid solution was found to form at temperature over 1200 °C without any indication of the intermediate phase. For the last sequence, the reaction between PbO and ZTMN (P+ZTMN) was proposed. A single phase PMN-PZT was obtained at 800 °C. This reaction gave PMN-PZT solid solution at considerably lower temperatures than those in the previous two methods.

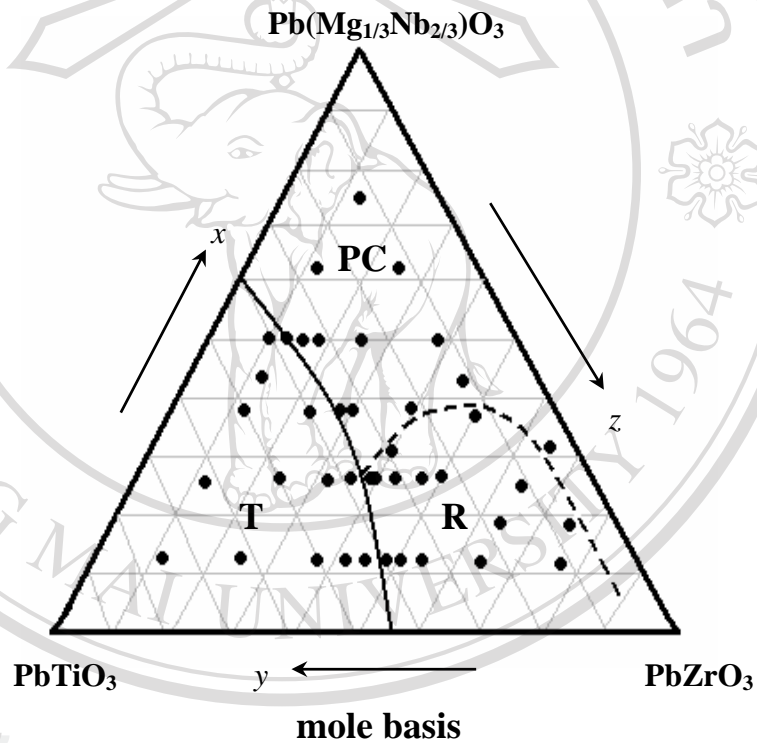


**Fig. 2.11** Compositions studied in the system  $x$ PMN- $y$ PT- $z$ PZ and phase boundaries at room temperature.<sup>76</sup> (Full descriptions are available in the abbreviations and symbols)

Villegas et al.<sup>79</sup> also studied the reaction mechanism of PMN-PT-PZ perovskite phase by employing mixtures of PbO, MgNb<sub>2</sub>O<sub>6</sub>, PbZrO<sub>3</sub>, PbTiO<sub>3</sub>

(P+MN+PZ+PT). Three steps of the reaction mechanism for the formation of PMN-PZT solid solution are suggested: i) decomposition of  $\text{MgNb}_2\text{O}_6$  by reacting with PbO at the range 350 °C-600 °C, ii) the formation of a B-site deficient pyrochlore phase  $\text{Pb}_2\text{Mg}_{1.33}\text{Nb}_{0.17}\text{O}_{5.50}$  at the temperature close to 650 °C and iii) the formation of perovskite phase PMN-PZT solid solution from the reaction of  $\text{Pb}_2\text{Mg}_{1.33}\text{Nb}_{0.17}\text{O}_{5.50}$  pyrochlore phase with MgO and PZT above 650 °C.

Although previous studies of PZT-PMN ceramics have been found in some works, little is known so far on the inter-relationships between composition, processing, phase formation, microstructure and dielectric properties. In the present work, therefore, attempts have been made to investigate this system in more details. Thus, the main work is an effort to determine such inter-relationship by employing the appropriate experimental techniques. Finally, the anticipation would be of obtaining the useful information for any kind of applications and would also fulfill the scientific understanding about this particular solid solution system.